REPORT - PROJECT 3

May 20, 2020

Ioanna Maria Lazarou
AST3310 - Astrophysical plasma and the interior of the stars
University of Oslo

1 Introduction

In the first two projects in this course, we have made a model of the interior of a star, where we have modelled the energy production by nuclear fusion in the core of a star. We have seen the energy transport throughout the interior of the star towards the surface, implementing both radiative and convective energy transport. These models were one dimensional and thus, limited in how realistic they are. In this project, we will start from ideal gas in hydrostatic equilibrium and temperature gradient slightly super adiabatic. We will model two dimensional convection in the upper layers of a star by using hydrodynamics.

2 Method

Initially, we assume that the system that everything is in hydrostatic equilibrium. This way we can set up initial conditions and test our system in a simplified situation, before invoking convection through a Gaussian perturbation in the initial temperature. The plasma is considered to be an ideal gas with constant mean molecular weight $\mu = 0.61$. The ideal gas assumption is more accurate as we are so close to the surface. In addition, an assumption is the constant gravitational acceleration over the hole computational volume, pointing towards the center of the star.

$$\vec{g} = -G\frac{M_\odot}{R_\odot^2}\hat{\mathbf{y}} = -g_y$$

where G is the gravitational constant. Here, we assume that the gravitational field strength is constant and equal to its value at the Sun's surface. The reason is that the radial distance of the area in the stars upper layers, is negligible compared to the Stars radius. As the box is so small and far from the center, we also have to mind the sign. The gravitational acceleration from a spherical mass is in the negative radial direction. The upper boundary of y should be at the surface of the star, thus $\hat{\mathbf{y}}$ is pointing in positive radial direction and $\vec{g}$ is negative. $g_y = GM_\odot R_\odot^{-2}$ can be defined to be the magnitude of the gravitational acceleration, dealing with the sign accordingly in the equations.

Since the gas in a star's upper layers behaves like a fluid, we'll be using hydrodynamics to model convection. In order to make the task at hand a bit more solvable we neglect internal friction and turbulence. Individual gas particles in a real gas have velocities on the form: $\vec{v} = \vec{u} + \vec{f}_i$, where $\vec{u}$ is the mean velocity of the particle (i.e. the velocity of the fluid as a whole) and $\vec{f}_i$ are velocities of the individual particles around the mean velocity. We will consider for simplification the velocity of the fluid as a whole $\vec{u}$. We need three equations to model convection. These are the continuity equation with no sources or sinks, governing the conservation of mass in the fluid. Next, the momentum equation for both x and y, excluding the viscous stress tensor but including gravity, as we want to conserve the total momentum of the fluid and the energy equation, as we need to conserve the internal energy of the fluid. These three laws are given as:

$$\frac{\partial \rho}{\partial t} + \vec{\nabla}\cdot(\rho\vec{u}) = 0 \tag{1}$$

$$\frac{\partial \rho\vec{u}}{\partial t} + \vec{\nabla}\cdot(\rho\vec{u}\vec{u}) = -\vec{\nabla}P + \rho\vec{g} \tag{2}$$

$$\frac{\partial e}{\partial t} + \vec{\nabla}\cdot(e\vec{u}) = -P\vec{\nabla}\cdot\vec{u}, \tag{3}$$

where ρ is the mass density, $\rho\vec{u}$ is the momentum density, e internal energy density (specific internal energy), P is the pressure and $\vec{g}$ is the gravitational field strength. We split the governing equations into components in x and y direction. By decomposing the velocity $\vec{u} = (u, w)$ and gradient $\vec{\nabla} = \left(\frac{\partial}{\partial x}, \frac{\partial}{\partial y}\right)$, we can rewrite eq. (1),eq. (2),eq. (3)into four equations. The continuity equation then becomes:

$$\frac{\partial \rho}{\partial t} = -\left(\frac{\partial}{\partial x}, \frac{\partial}{\partial y}\right)\cdot(\rho u, \rho w) = -\frac{\partial \rho u}{\partial x} - \frac{\partial \rho w}{\partial y}. \tag{4}$$

The volume of our system is in 2D and we must divide the star's volume into cells, where for each of the variables used in the calculations each cell is approximated by one value. We create cubic cells of size $\Delta x \times \Delta y$. We then choose respectively a computation volume of nx and ny cells in x and y direction. The volume is positioned with the top at the surface of the star, with y direction radially from the center (vertical) and x along the surface (horizontal). We let x enclose $12\,\mathrm{Mm}$ and y $4\,\mathrm{Mm}$, with $y = 4\,\mathrm{Mm}$ at the surface of the star and $y = 0$ at the bottom of the box. The computation volume is much less than the volume of the star and located far from the center. Therefore, the horizontal and vertical component are approximated as perpendicular. Each cell holds a position described in the volume as:

$$(x, y) = (i\Delta x, j\Delta y) \quad \text{with} \quad \begin{matrix} i \in [0, nx-1] \\ j \in [0, ny-1]. \end{matrix}$$

The momentum equation is split in two, one horizontal and one vertical component. Here Einstein's summation convention is applied to simplify the notation, v_i is the i-th compo-

nent of the velocity $\vec{u}$, and $i, j \in [x, y]$.

$$\frac{\partial \rho v_i}{\partial t} = -\frac{\partial}{\partial x_j}\left(\rho v_i v_j\right) - \frac{\partial P}{\partial x_i} + \rho g_i$$

$$\underline{\text{for} \quad i = x, \quad j = x, y, \quad g_x = 0}$$

$$\Rightarrow \frac{\partial \rho u}{\partial t} = -\frac{\partial \rho u^2}{\partial x} - \frac{\partial \rho u w}{\partial y} - \frac{\partial P}{\partial x} \tag{5}$$

$$\underline{\text{for} \quad i = y, \quad j = x, y, \quad g_y = g_y}$$

$$\Rightarrow \frac{\partial \rho w}{\partial t} = -\frac{\partial \rho w^2}{\partial y} - \frac{\partial \rho u w}{\partial x} - \frac{\partial P}{\partial y} - \rho g_y. \tag{6}$$

Where gravity is only in the vertical direction. For the energy equation, using Einstein's summation convention we have:

$$\frac{\partial e}{\partial t} + \frac{\partial e v_i}{\partial x_i} = -P\frac{\partial v_i}{\partial x_i} \qquad i = x, y$$

$$\frac{\partial e}{\partial t} + \frac{\partial e u}{\partial x} + \frac{\partial e w}{\partial y} = -P\left(\frac{\partial u}{\partial x} + \frac{\partial w}{\partial y}\right)$$

$$\Rightarrow \frac{\partial e}{\partial t} = -\frac{\partial e u}{\partial x} - \frac{\partial e w}{\partial y} - P\left(\frac{\partial u}{\partial x} + \frac{\partial w}{\partial y}\right). \tag{7}$$

The initial gradients for each parameter are in the vertical direction only. From project 2, the double logarithmic gradient is:

$$\nabla = \frac{\partial \ln T}{\partial \ln P} = \frac{2}{5} + \mathrm{d}\nabla \tag{8}$$

where $\mathrm{d}\nabla$ is some small positive perturbation from the adiabatic gradient of $2/5$. In this project, we choose a value $\mathrm{d}\nabla = 1 \times 10^{-4}$ and the gradient is assumed to be constant. Moreover,we know the values of the temperature and pressure from the Sun's photo-sphere: $T_\odot = 5778\,\mathrm{K}$ and $P_\odot = 1.8 \times 10^8\,\mathrm{Pa}$. We can find the initial conditions for T and P in the hole box for $n = 0$, $i \in [0, nx - 1]$ and $j = ny - 1$. First, we rewrite the logarithmic gradient to find a separable equation for the temperature in the hole box as a function of height y. We need to use two expressions for the equation of state of an ideal gas, one relating the pressure and energy and one relating the energy with density and temperature.

$$P = (\gamma - 1)e$$

$$e = \frac{1}{(\gamma - 1)}\frac{\rho}{\mu m_u} k_B T$$

where m_u is the unit atomic mass in kg and $\gamma = \frac{f+2}{f} = \frac{5}{3}$ is a thermodynamic constant, the adiabatic index, determined by the degrees of freedom of the particles in the gas, here $f = 3$.

Using the product rule and the equations of state we find:

$$\nabla = \frac{P}{T}\frac{\partial y}{\partial P}\frac{\partial T}{\partial y} \quad \text{where} \quad P = \frac{\rho}{\mu m_u} k_B T, \quad \frac{\partial y}{\partial P} = -\frac{1}{\rho g_y}$$

$$= -\frac{k_B}{\mu m_u g_y}\frac{\partial T}{\partial y}$$

From the initial temperature at the surface $y_{\max}$, denoted $T_\odot$, we can find the temperature at height y by integrating both sides.

$$\int_T^{T_\odot} \mathrm{d}T = -\int_y^{y_{\max}} \frac{\mu m_u g_y}{k_B} \nabla \,\mathrm{d}y$$

$$\Rightarrow T(y) = T_\odot - \frac{\mu m_u g_y}{k_B}\nabla\left(y - y_{\max}\right). \tag{9}$$

We can find initial pressure with the initial temperature by using the state equations again.

$$P(y) = (\gamma - 1)e = \frac{\rho}{\mu m_u} k_B T(y) \quad \Big| \cdot \frac{g_y}{g_y}$$

$$= -\frac{\partial P}{\partial y}\frac{k_B}{\mu m_u g_y}\left(T_\odot - \frac{\mu m_u g_y}{k_B}\nabla\left(y - y_{\max}\right)\right)$$

$$= -\frac{\partial P}{\partial y}\left(\frac{k_B T_\odot}{\mu m_u g_y} - \nabla(y - y_{\max})\right). \tag{10}$$

and for simplicity:

$$\beta(y) = \frac{k_B T_\odot}{\mu m_u g_y} - \nabla(y - y_{\max})$$

$$\frac{\partial \beta}{\partial y} = -\nabla, \quad \beta(y_{\max}) = \beta_0 = \frac{k_B T_\odot}{\mu m_u g_y}$$

Inserting into eq. (10) gives

$$P = -\frac{\partial P}{\partial y}\beta \Rightarrow \frac{\mathrm{d}P}{P} = \frac{\mathrm{d}\beta}{\nabla\beta}.$$

We use the integration technique once again:

$$\int_P^{P_\odot} \frac{\mathrm{d}P}{P} = \int_\beta^{\beta_0} \frac{\mathrm{d}\beta}{\nabla\beta}$$

$$\ln\left(\frac{P_\odot}{P}\right) = \frac{1}{\nabla}\ln\left(\frac{\beta_0}{\beta}\right)$$

$$\Rightarrow P(y) = P_\odot\left(\frac{\beta}{\beta_0}\right)^{1/\nabla} \tag{11}$$

and in last part, we use the the exponential and logarithmic properties of functions.

With the defined initial pressure and temperature we can find the initial density and energy, by using the equations of state. In the final version, we apply the Gaussian perturba-

tion before initializing ρ and e.

$$e(y) = \frac{P(y)}{(\gamma - 1)} \tag{12}$$

$$\rho(y) = e(y)(\gamma - 1)\frac{\mu m_u}{k_B T(y)}. \tag{13}$$

We also have some boundary conditions for u,ρ and e. As about the index notation, Q, n indicate the time step and i, j indicate the position in the grid of the quantity Q. We have to apply certain limiting conditions because the computational volume has discontinuous boundaries. First, we apply horizontal boundary conditions periodically, leaving our volume to be continuous in the x-direction. It makes sense, as we assume that the sides of the computational volume contain neighboring boxes[1]. For the vertical boundaries, we only need boundary conditions for the four primary variables (ρ, e, u, w). In the following, each vertical boundary is described by indices $i \in [0, nx-1]$ and $j = 0$ for bottom and $j = ny-1$ for the surface, and used for all times n. At the bottom and top of our box, the vertical velocity w should be zero. Because we use the continuity equation without sources or sinks, this is valid in order to prevent mass from leaking out into the photosphere, and in through the bottom of the box.

$$w_{i,j} = 0. \tag{14}$$

Moreover, the vertical gradient of the horizontal velocity u must also be zero at the boundary. We need to find an expression for $u_{i,j}$ at the boundary. We can use the forward and backwards approximations for the partial derivative and solve for $u_{i,j}$:

$$\frac{\partial u}{\partial y} = \frac{-u_{i,j+2} + 4u_{i,j+1} - 3u_{i,j}}{2\Delta y} = 0$$
$$\frac{\partial u}{\partial y} = \frac{u_{i,j-2} - 4u_{i,j-1} + 3u_{i,j}}{2\Delta y} = 0,$$

We have now two different expressions, one for the top and one for bottom boundary.

$$\begin{aligned} u_{i,0} &= \frac{4u_{i,1} - u_{i,2}}{3} \\ u_{i,ny-1} &= \frac{4u_{i,ny-2} - u_{i,ny-3}}{3}. \end{aligned} \tag{15}$$

Last, we need boundary conditions for the energy and density. The system must be in hydrostatic equilibrium along the border. We use the equations of state and

$$\frac{\partial P}{\partial y} = -\rho g_y \tag{16}$$

and we find an expression for the vertical gradient of the energy:

$$\frac{\partial P}{\partial y} = (\gamma - 1)\frac{\partial e}{\partial y} = -\rho g_y$$
$$\text{inserting} \quad \rho = (\gamma - 1)\frac{\mu m_u}{k_B T} e \quad \text{gives}$$
$$\frac{\partial e}{\partial y} = -g_y \frac{\mu m_u}{k_B T} e.$$

We use the same technique as for the horizontal velocity but this time we set the approximation equal to the gradient for the energy. By using forward differentiation for $j = 0$:

$$\frac{\partial e}{\partial y}_{i,0} = \frac{-e_{i,2} + 4e_{i,1} - 3e_{i,0}}{2\Delta y} = -g_y \frac{\mu m_u}{k_B T_{i,0}} e_{i,0}$$
$$4e_{i,1} - e_{i,2} = e_{i,0}\left(3 - 2\Delta y g_y \frac{\mu m_u}{k_B T_{i,0}}\right)$$

In the same way, using backwards differentiation for $j = ny-1$, the boundary conditions for the energy:

$$\begin{aligned} e_{i,0} &= \frac{4e_{i,1} - e_{i,2}}{3 - 2\Delta y g_y \frac{\mu m_u}{k_B T_{i,0}}} \\ e_{i,ny-1} &= \frac{4e_{i,ny-2} - e_{i,ny-3}}{3 + 2\Delta y g_y \frac{\mu m_u}{k_B T_{i,ny-1}}}. \end{aligned} \tag{17}$$

With values for the energy at the boundary, using the equations of state we find the density:

$$\begin{aligned} \rho_{i,0} &= (\gamma - 1)\frac{\mu m_u}{k_B T_{i,0}} e_{i,0} \\ \rho_{i,ny-1} &= (\gamma - 1)\frac{\mu m_u}{k_B T_{i,ny-1}} e_{i,ny-1}. \end{aligned} \tag{18}$$

Solving the equations numerically, from eq. (4) -eq. (7), as the flow is not constant, we expand the velocity terms using the product rule.

[1] This condition is implemented through the numerical differential solvers.

$$\begin{aligned}\frac{\partial \rho}{\partial t} &= -\rho\left(\frac{\partial u}{\partial x}+\frac{\partial w}{\partial y}\right)\\ &\quad - u\frac{\partial \rho}{\partial x} - w\frac{\partial \rho}{\partial y}\end{aligned} \tag{19}$$

$$\begin{aligned}\frac{\partial \rho u}{\partial t} &= -\rho u\left(\frac{\partial u}{\partial x}+\frac{\partial w}{\partial x}\right)\\ &\quad - u\frac{\partial \rho u}{\partial x} - w\frac{\partial \rho u}{\partial y}\\ &\quad - \frac{\partial P}{\partial y}\end{aligned} \tag{20}$$

$$\begin{aligned}\left[\frac{\partial \rho w}{\partial t}\right]^n_{i,j} &= -[\rho w]^n_{i,j}\left(\left[\frac{\partial w}{\partial y}\right]^n_{i,j}+\left[\frac{\partial u}{\partial x}\right]^n_{i,j}\right)\\ &\quad - [w]^n_{i,j}\left[\frac{\partial \rho w}{\partial y}\right]^n_{i,j} - [u]^n_{i,j}\left[\frac{\partial \rho w}{\partial x}\right]^n_{i,j}\\ &\quad - \left[\frac{\partial P}{\partial y}\right]^n_{i,j} + [\rho g_y]^n_{i,j}.\end{aligned} \tag{21}$$

$$\begin{aligned}\left[\frac{\partial e}{\partial t}\right]^n_{i,j} &= -[e]^n_{i,j}\left(\left[\frac{\partial u}{\partial x}\right]^n_{i,j}+\left[\frac{\partial w}{\partial y}\right]^n_{i,j}\right)\\ &\quad - [P]^n_{i,j}\left(\frac{\partial u}{\partial x}+\frac{\partial w}{\partial y}\right)\\ &\quad - u\frac{\partial e}{\partial x} - w\frac{\partial e}{\partial y}\end{aligned} \tag{22}$$

We have to approximate the derivatives in the governing equations by finite difference methods to solve our equations in the defined grid of cells. For stability, we implement two different explicit methods for the spatial terms. Q denotes to be any quantity we need to spatially differentiate in eq. (19), eq. (20), eq. (21), eq. (22) The Forward Time Centred Space scheme which will be used whenever viable for non transport terms, which are not multiplied by the flow (u or w):

$$\begin{aligned}\frac{\partial Q}{\partial x} &= \frac{Q^n_{i+1,j} - Q^n_{i-1,j}}{2\Delta x}\\ \frac{\partial Q}{\partial y} &= \frac{Q^n_{i,j+1} - Q^n_{i,j-1}}{2\Delta y}\end{aligned} \tag{23}$$

Next, for the transport terms, we use the upwind differencing scheme. This method depends on the direction of the flow in the actual cell we are calculating in. With positive flow we use backward differentiation, we use information from the cell before the current cell to find the next value. For negative flow we do the opposite. This is more accurate since we know how the previous cell is moving towards the current cell. Terms multiplied by the flow u:

$$\begin{aligned}\frac{\partial Q}{\partial x} &= \begin{cases}\frac{Q^n_{i,j}-Q_{i-1,j}}{\Delta x} & \text{if} \quad u \geq 0\\ \frac{Q^n_{i+1,j}-Q_{i,j}}{\Delta x} & \text{if} \quad u < 0\end{cases}\\ \frac{\partial Q}{\partial y} &= \begin{cases}\frac{Q^n_{i,j}-Q_{i,j-1}}{\Delta y} & \text{if} \quad u \geq 0\\ \frac{Q^n_{i,j+1}-Q_{i,j}}{\Delta y} & \text{if} \quad u < 0\end{cases}\end{aligned} \tag{24}$$

The type of differentiation is determined by the sign of w instead of u in the exact same fashion for the terms, multiplied by the w flow.

In order to solve these four equations numerically we need discretization of the equations. We can now find values for each time derivative. We find an optimal time step Δt for each integration loop, based on the largest valued time derivative. In this way, the relative change in density and energy is below a set tolerance. The same goes for the flow parameters, no velocity moves a cell's content past a hole grid point. The tolerance is determined using the parameter $p = 1 \times 10^{-2}$. This demands that $\Delta t = \delta \cdot p$, where δ is the largest relative change in any of the primary variables. In the next time step we find the new value. We expand the temporal terms in the equations using forward time, and then solve for $Q^{n+1}_{i,j}$:

$$\frac{\partial Q}{\partial t} = \frac{Q^{n+1}_{i,j} - Q^n_{i,j}}{\Delta t} \tag{25}$$

$$Q^{n+1}_{i,j} = Q^n_{i,j} + \frac{\partial Q}{\partial t}\Delta t \tag{26}$$

provided that in the current time phase we have the time derivative.

Following the code in the hydro solver, the numerical solver in use we lay out the algorithm in order to solve our system. The aim is to evolve each primary variable one step in time, and use the new values to update temperature and pressure in the following time step. In the first time step we know each variables value in the hole volume from the initial conditions. The steps we follow are: 1)To save computation time, at the start of each integration loop to, we find the direction of flow for the hole box, which is in use in all the following upwind differentials. 2)We then find each of the time derivatives (or right-hand-sides) of eqs. (19) to (22) using the appropriate numerical method on each term. 3)With the time derivatives we can find the optimal time step to evolve our variables and use eq. (26) to find the value in the next time step for ρ and e. We know the time derivative of ρu and ρw, not u and w them self. After we find the value for ρ^{n+1}, the next flow is found by dividing eq. (26) by ρ^{n+1}

$$w^{n+1}_{i,j} = \frac{\rho w + \frac{\partial \rho w}{\partial t}\Delta t}{\rho^{n+1}_{i,j}} \tag{27}$$

then inserting eq. (21) for the time derivative. 4)Before the next step , it is necessary that we apply the boundary conditions. After each primary variable has been modified we apply the boundary conditions. It will update the previous measured values on the numerical volume's upper and lower horizontal boundaries. 5) The last step is to adjust the pressure and temperature to the new time step, after application

of the boundary conditions. To find the correct distribution of T and P we again use the equations of state:

$$\begin{aligned} P_{i,j}^{n+1} &= (\gamma-1)e_{i,j}^{n+1} \\ T_{i,j}^{n+1} &= (\gamma-1)e_{i,j}^{n+1}\frac{\mu m_u}{k_B \rho_{i,j}^{n+1}}. \end{aligned} \tag{28}$$

In order to start convection in our hydrostatic equilibrium situation,to provoke the gas to become convectively unstable, we perturb the initial temperature distribution with a Gaussian perturbation. The perturbation acts like a circular blob of gas, or a parcel, with higher temperature than the surroundings. This is done during initialization, before solving the equations. First the initialazation of the energy and density takew place. Then, after the calculation of the initial temperature and pressure distribution using eqs. (9) and (11), the perturbation is added to the temperature values. The perturbation, λ, is created as a 2D Gaussian bell mesh grid:

$$\lambda = \exp\left[-\left(\frac{x-x_{avg}}{\sigma_x}\right)^2 - \left(\frac{y-y_{avg}}{\sigma_y}\right)^2\right] \tag{29}$$

where x_{avg} and y_{avg} marks the center of the perturbation, x and y spans the computational volume. σ_x and σ_y is the full width at half maximum of the perturbation.

Fist we perform a single positive perturbation in the center of the computational box, $x_{avg} = 6\,\mathrm{Mm}$ and $y_{avg} = 2\,\mathrm{Mm}$. We choose equal standard deviations in both directions for a circular bell function, $\sigma_x = \sigma_y = 8\times10^5$. Then λ is added to the initial temperature as we can see below. α controls the amplitude of the perturbation.

$$T_{\text{perturbed}} = T_{\text{inti}} + \alpha T_\odot \lambda$$

Any number of perturbations can be added, equally spaced along the horizontal direction, to see how they influence each other. If there are multiple perturbations we can chose alternating positive and negative α values. Thus, each perturbation creates a rising and sinking parcel, with higher and lower temperature than the surroundings.

The order of operations was very important and here is a brief summary of how the whole progress was dealt with. We started on how to implement the initialization of all the variables, without perturbation. These equations are mainly governed by the equations of state and hydrostatic equilibrium. an 1D plot of the vertical component of each variable(sanity init) was implemented to benchmark that the initial distributions made physically sense. This was to verify that all the variables were increasing from the surface of the cell down to the bottom. All the methods for differentiation were implemented together with the method for finding flow directions. This way we incorporate periodic boundary conditions in both directions and we calculate the differentials over the hole mesh grid.

Next, the boundary conditions methods were implemented. The order of operations is important for the density and energy. We first calculate the boundary values for the energy by using eq. (17), and then we use the new updated values in eq. (18) to set the values for the density.

What followed was to find the optimal time step. To remove possibilities of zero divisions, we removed all cases of infinity in the calculation of δ, and made it strictly positive. In order to prevent the calculation to go too slow, it was important to implement a minimum time step of $\Delta t = 1\times10^{-7}\,\mathrm{s}$. Also, we implemented a max time step of $\Delta t = 0.1\,\mathrm{s}$ for the hydrostatic case where the relative change in variables is very low.

After that, focus was given on the solver. First, it is calculating the energy and density. Then it is the flow, using appropriate values for the density in the denominator and numerator as demonstrated in eq. (27). Next we apply the boundary conditions, importantly before calculations of temperature and pressure. With the completed solver we test the code against our main benchmark, hydrostatic equilibrium(Sanity test, sanity animate). We run the simulation over $60\,\mathrm{s}$, with unperturbed initial conditions. As we know, the hydro-dynamical system should be unchanging when it is in hydrostatic equilibrium. If everything is correct, we should have a static situation, even though the system is so unstable.

Next, the perturbation was applied in the initial conditions, and the final simulations were performed. In this code, in the initial implementation, we made a single positive perturbation in the middle of the computational volume so we can test whether the method worked, before extending the method to create arbitrary many alternating positive and negative perturbations along the x-direction. The last addition to the code is animating the convective flux through the volume(basic flux animate, snap). We choose to look at the averaged convective flux through each cross-section of the volume in the vertical direction. This way we can see at which depths, and at what times, most of the energy transportation is happening.

3 Results

The final result from our simulations are movies and snapshots of the 2D distributions of the different variables, focusing on the temperature. To display the convection cells in

detail, we use quite dense and small arrow-scales, while still being able to run the simulation far enough to see where it broke down. Due to the fact that our numerical method is so unstable, we can not simulate the situation long enough for the temperature distribution to change much noticeably. We interpret the results by looking at the fields of induced velocity which would eventually cause other variables to shift around. We can see snapshots of the time evolution for the basic situation in figs. 1a to 1d. This is the most basic case of perturbation(basic animate), a single positive perturbation at the center of the distribution. In these figures, we can see the behavior as expected from a hot parcel of gas. Simultaneously, we can see in fig. 2 how the convective flux is related to the 2D distributions. The behaviour of the gas blob follow the known hydrodynamical and thermodynamical properties it should have. But in order to make this model more realistic one could have included the stress tensor of the fluid and viscosity so as to allow for turbulence to play a role. Also the simulation could be further improved using higher order numerical methods, or a smaller accuracy parameter in the dynamical time step, in order to improve accuracy. Also one could use a finer grid improving the accuracy of the gradients found numerically. However, considering our simplified model does not include viscosity nor advanced higher order methods, it behaves quite realistically.

In figure 1a, we see the initial distribution, after the perturbation is added. The bell shaped increase in the temperature causes the color plot to increase, with a smooth bulk in the middle. It follows a normal distribution in both directions. From the initialization, we have close to zero velocity field. This is also evident in fig. 2a, where we see a close to zero flux.

As the initial velocity is set to zero, the velocity field takes some time to catch up. In 1b we can see the situation after about one minute. We can see how the increased temperature causes a positive flow in the vertical direction, consistent with how we know that hot gas rises in a surrounding cooler medium. It is explained by the equations of state, where we know the temperature and density to be linearly inverse. The surrounding medium is initialized in hydrostatic equilibrium, so it will not be accelerated, and the velocity field stays zero. The hotter gas will have a lower density, and therefore is pulled down less by the gravitational attraction breaking the hydrostatic equilibrium. The lower gravitational pull causes a net positive acceleration, inducing a positive velocity field, which eventually results in the parcel rising through the medium. We can also see that we are close to the maximum in convective flux since the velocity is in positive direction. The maximum is located below the middle depth as the density is higher at the bottom of the box.

Then, at time `02:35` in 1c, the parcel has reached the surface, which is consistent with hot granules as we observe them on the sun. The hot gas will radiate away energy, and so is cooled off. We notice that the maximum of the vertical flux moving to a higher y-value. We see how the velocity field starts getting a horizontal component near the surface. This is caused by the hot gas still rising below it, pushing the cooled gas to each side. The velocity field is still mostly in the middle and the upper part of the parcel.

In 1d, the convection circle is completed. The cooled off gas falls back down, by the same argument we used for it rising initially, only reversed. The cooler gas has a higher density, and is therefore accelerated down again. It is then warmed back up to the surrounding temperature at the bottom of the computational volume. The cooled gas still falling above it causes horizontal velocity to each side eventually rejoining the velocity field in the middle which is still in positive vertical direction. The averaged vertical flux is all negative at this point, as there are so many more cells with a negative vertical flow than positive. If we were able to simulate the situation for longer, we would see how the convective flux start changing back to being positive. This process will oscillate back and forth from being negative to positive, as parcels rise and falls back down.

4 Conclusion

The aim of this project was to simulate the convection inside the upper layers of a star. We did that by starting from the laws of mass, momentum, and energy conservation. These where then discretized in order to make an updating algorithm for the primary variables density ρ, velocities u and w as well as the internal energy density e. Initial and boundary conditions where then found under the assumption of hydrostatic equilibrium. After the sanity check at maintaining hydrostatic equilibrium over the course of a 60 sec simulation, we added a Gaussian temperature perturbation to make the gas become connectively unstable. During the first few hundred seconds before numerical instabilities took over, the resulting simulation of temperature and fluid velocity was quite stable. Also, the behavior of the fluids followed well known physics predictions.

We have tried to provide informative visualization of the quantities involved. We have studied a highly unstable system of partial differential equations, and how to solve them numerically. We have also gained new and greater insight into how the state equations are combined with all of these quantities. The visualised results, in the form of 2D convec-

tion, have been helpful in understanding more in-depth the theory covered in the course. We learned about boundary conditions and how critical they are to constrained systems. Finding the right boundary conditions has been an fascinating and challenging operation. Working with subtly different boundaries has been informative on how those can affect the system's behaviour.

There were several difficulties in this project. The biggest was actually starting the project, with a lot of information about the system and the problem to absorb. We had to figure out how to deal with the system and the model in a physically, numerical and graphical sense. Through the direction of gravity and the vertical pressure gradient, we established how the situation had to behave physically. Lastly, it was challenging to follow the logic behind the provided visualization module, which flips the vertical axis. After obtaining some understanding of required concepts, the rest of the project became a bit easier.

In this model, turbulence was not simulated. This could be done by including the viscous stress tensor in our governing equation for the momentum. The stress tensor governs internal friction in the dynamical system. The friction is present between neighboring flow streams of mass with different velocities.

Overall, it was quite enjoyable to spend time on this, and both previous projects. The educators of this course were really motivating. The most interesting part of this project was simulating gas convection, as it takes place in the outer parts of the Sun, and many stars like it.

Figure 1: Distribution of temperature shown in colors, velocity vector field shown as arrows. Figures 1a to 1d shows the time evolution of the system. Initial conditions are perturbed with a single positive circular Gaussian perturbation, which acts as a parcel of hot gas rising through the medium. The hot pocket eventually reach the surface and cools down, before it is pushed to the side and falls back down, creating a 2D convection cell.

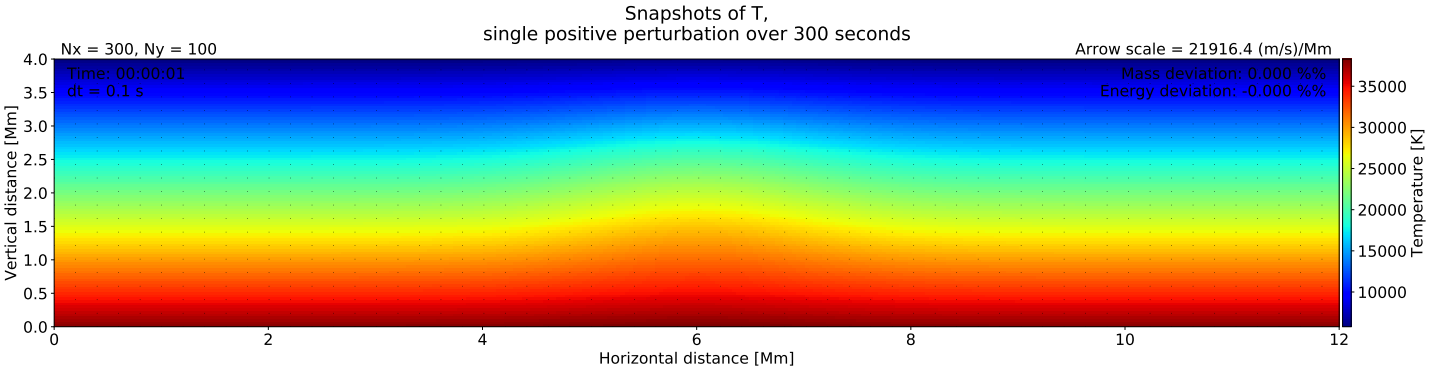

(a) The initial distribution, before the perturbation give non-zero velocity. The increased temperature is visible as the bulk in the y-direction. There is a zero (or close to zero) value of the velocity field over the hole volume.

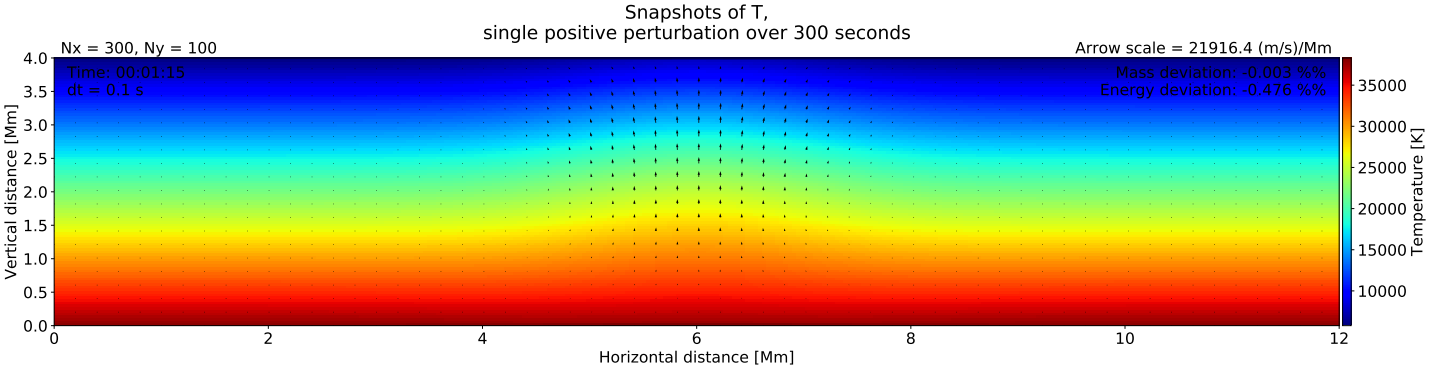

(b) About one minute into the simulation. Here we see the effects of the hot parcel, giving rise to positive vertical flow in the center of the box pushing the parcel towards the surface.

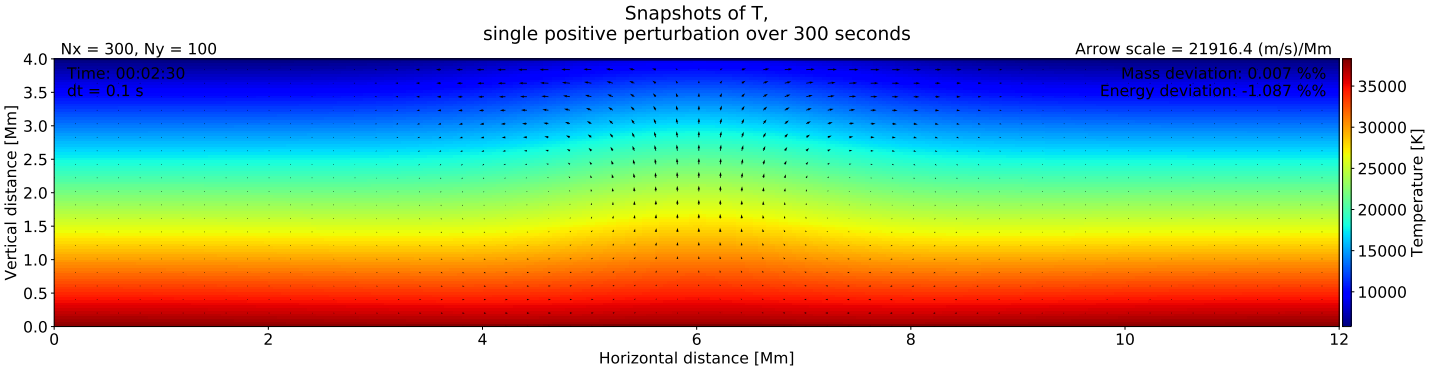

(c) 02 : 15 into the simulation and we can see how the medium is pushed out to each side horizontally when the parcel reaches the surface. This is as expected, as we know these can be observed as granules on the Sun.

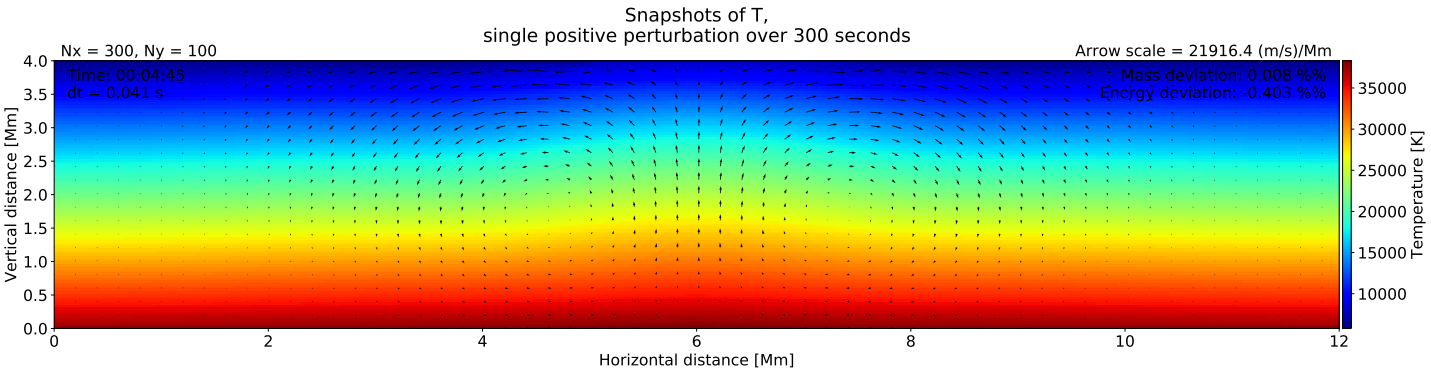

(d) The last snapshot from the simulation, at 04 : 45. Here we see how the cooled gas that has been pushed to the sides falls back down. This process concludes the convection circle, and is visible in the pleasant circular velocity fields at both sides of central hot rising region.

Figure 2: Horizontally averaged vertical energy flux of the basic perturbation situation shown in fig. 1, snapshots of corresponding times in figs. 2a to 2d. Here we see how the vertical energy transportation changes with the changes in velocity fields. The large amplitude of the flux, this is caused by the very large value of e.

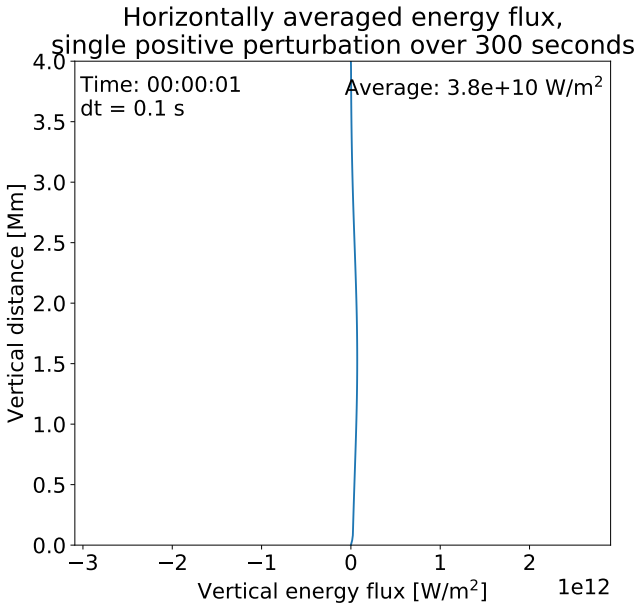

(a) Initial situation, close to hydrostatic equilibrium.

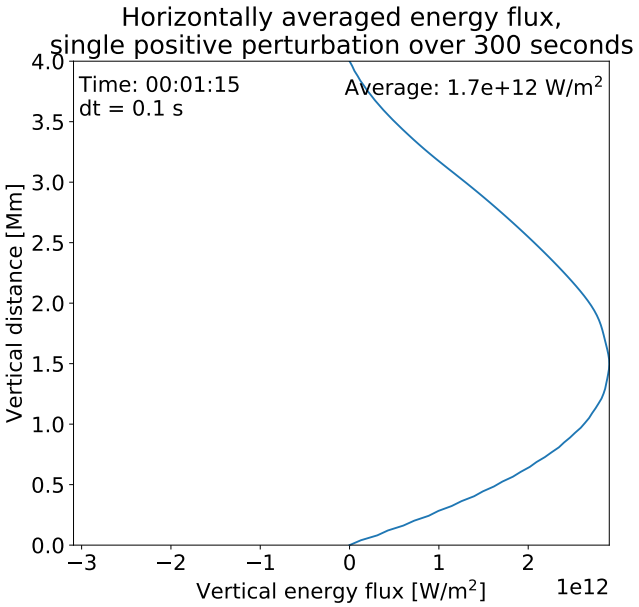

(b) Close to the maximum of the flux, at time 01 : 15. Consistent with what we saw in fig. 1b, here we still only have positive vertical flow, causing a large positive vertical convective flux.

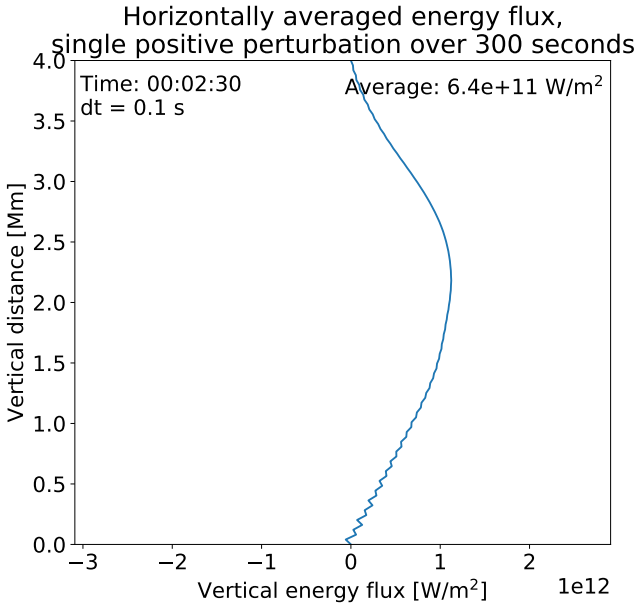

(c) 2 minutes and 30 seconds in, and we see the maximum of the flux being moved to a higher y-value. Caused by the increase in velocity field, which increases in a circular path before it completes itself, as seen in fig. 1. Also, as the parcel rises through the medium, we get higher values of e closer to the surface.

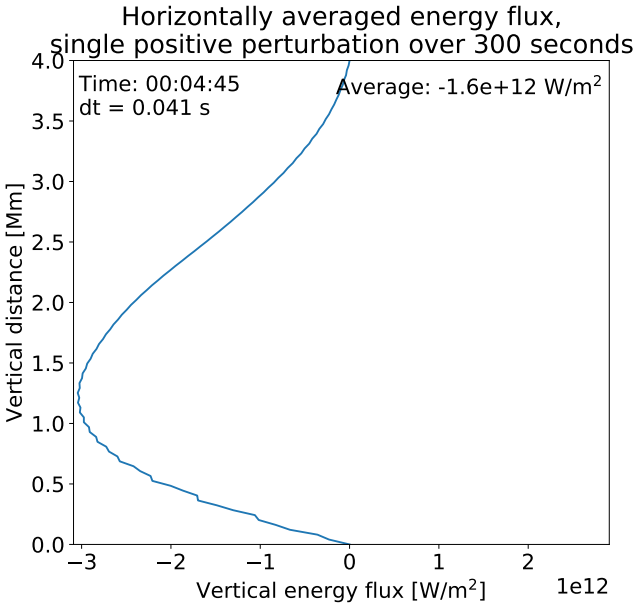

(d) Finally we have a minimum value of the flux, being negative at all depths. This is caused by the parcel falling back down at both sides of the rising pocket. Now the areas where negative flow is happening are so much larger than the positive part, and so the averaged flux across each depth is negative.

Figure 3: Distribution of temperature shown in colors, velocity vector field shown as arrows. Figures 3a and 3b,fig. 3c shows the time evolution of the system. Initial conditions are perturbed with 5 circular Gaussian perturbations equally spaced along x-direction, with altering sign of the perturbation. This creates both parcels rising and falling in the medium, accelerating the process of completing the convection cycles. One can see how the system starts of at rest, after which the cold blobs start sinking and the warm blobs start rising. After a while then there are several convection cells forming.

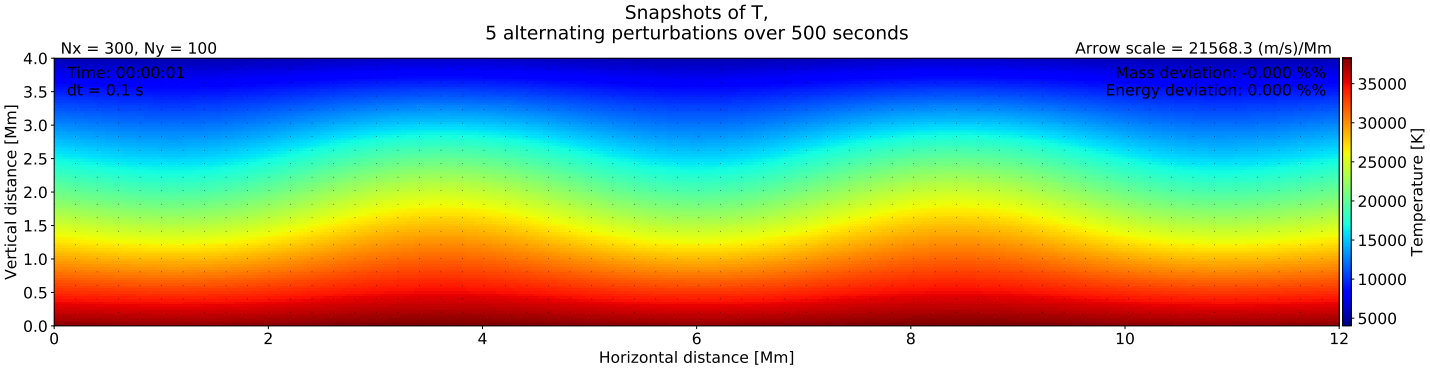

(a) Initial temperature distribution. Compared to fig. 1a the perturbation seems larger, but that is only caused by the neighboring negative perturbation.

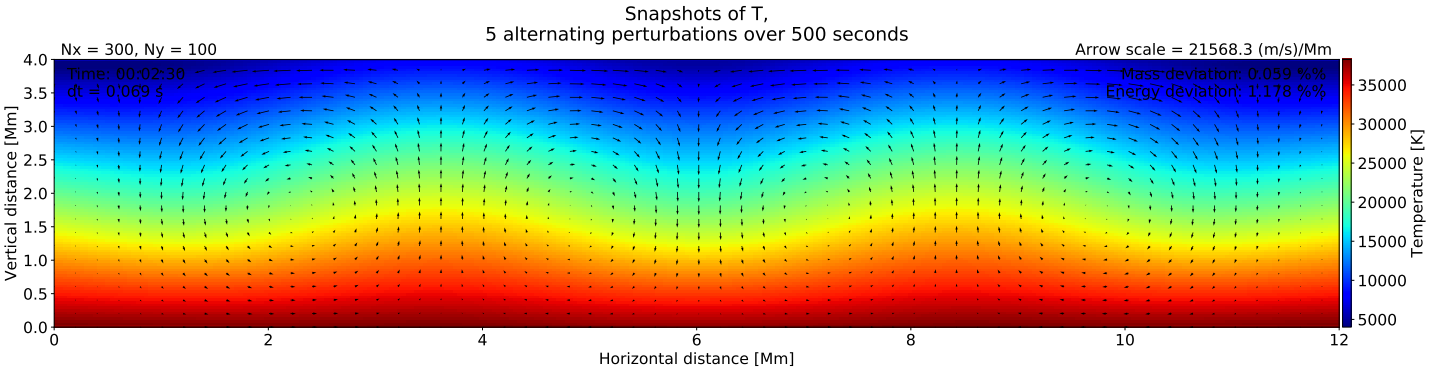

(b) 2 minutes and 30 seconds into the simulation and we have rising and sinking parcels. We can see compared to fig. 1c the process of completing the convection cells are already visible.

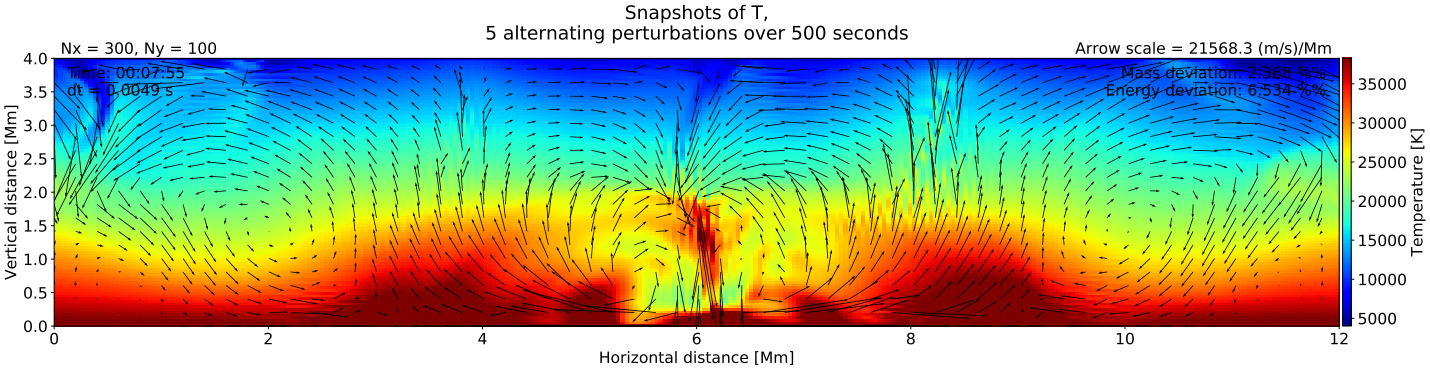

(c) 7 minutes and 55 seconds we can see that the convection cells are fully formed. Here we show how the simulation starts to break down after a while. We can see some strange behavior, present near the edges of our computational volume, especially in each corner and at the top middle area where the rising parcels meet. We can see how our current simulations struggles with this near the edges where the boundary conditions creates shock waves of unphsycial behavior, and where there are large relative differences in the velocity field over small areas.